JOURNAL OF CATALYSIS 54, 66–80 (1978)

Isotopic Mixing in Carbon Monoxide Catalyzed by Zinc Oxide

G. CARNISIO,* F. GARBASSI,* G. PETRINI,*,[1] AND G. PARRAVANO†,[2]

* *Donegani Research Institute, I-28100 Novara, Italy, and* † *Department of Chemical Engineering, University of Michigan, Ann Arbor, Michigan 48109*

Received October 24, 1977; revised March 6, 1978

The rate of the isotopic mixing in CO has been studied at 300°C, for CO partial pressures from 6 to 100 Torr and a total pressure of 250 Torr on ZnO catalysts. Significant deviations from a first-order rate in p_{CO} were found. The rate of oxygen exchange between ZnO and gas-phase CO was also measured and the results were employed to calculate the fraction of surface sites active for the CO isotopic mixing. Values on the order of 0.001 were found. The turnover rate and surface collision efficiency varied between 0.7 and 107 min^{-1} and 0.13 and 2.24×10^{-8}, respectively. H_2 additions to CO increased the rate of isotopic mixing, whereas the rate of $H_2 + D_2$ was decreased by the presence of CO. The $H_2 + D_2$ rate was faster than that of isotopic mixing in CO, but as the ratio p_{H_2}/p_{CO} decreased the rates became about equal.

It is argued that on ZnO samples, in which the rate of CO isotopic mixing and the rate of ZnO–CO oxygen exchange were influenced in a similar manner by the CO pressure, the isotopic mixing in CO took place via the ZnO oxygen, while oxide oxygen participation was not kinetically significant for ZnO samples in which the two reactions had different kinetics. The crucial factor controlling the path followed by the isotopic mixing in CO seems to be the surface Zn/O ratio, since a close correlation was found between the former and the reaction kinetics of the CO isotopic mixing reaction. Solid-state conditions which may vary the Zn/O surface ratio (foreign additions) are indicated. The implications of these findings to the problem of product selectivity from CO–H_2 mixtures reacting on metal oxide surfaces are discussed.

Product distribution in catalytically reacting mixtures of CO and H_2 is governed by several physicochemical conditions. Among these conditions are the nature and stoichiometry of CO adsorption, the structure of the adsorbate, and the coordination between the adsorbate structure and surface sites. Information on the nature of CO adsorption is particularly important when considering metal oxide catalysts, the surfaces of which possess a wide range of sites for adsorption and reaction. There is already a considerable amount of information on the adsorption modes of CO at metal oxide surfaces. With few exceptions (*1*) this information was obtained from observations on static and/or dynamic adsorption effects (ir, LEED, ESCA, adsorption volumetry), without concomitant measurements on the reactivity of each adsorption mode. The correlation between adsorption and reactivity was generally suggested by observations on additional properties of the reacting system.

To clarify the relation between the nature of the adsorption and its reactivity, measurements on both properties must be carried out simultaneously, and the effect on them of various operational factors must be directly assessed. For this purpose, isotopic exchange reactions are particularly

[1] To whom correspondence should be sent.

[2] Deceased on April 1, 1978.

0021-9517/78/0541-0066$02.00/0

suitable since they provide information simultaneously on the thermodynamics and kinetics of adsorption, thus enabling one to establish a direct link between the nature of the adsorption isotherm and the reaction efficiency.

To examine the reactive adsorption of CO we have employed the isotopic mixing reaction,

$$^{13}C^{16}O(g) + {}^{12}C^{18}O(g) \rightarrow {}^{13}C^{18}O(g) + {}^{12}C^{16}O(g), \quad (1)$$

where g refers to gas phase, and observed the rate of reaction (1) as a function of the partial pressure of CO, in the presence and absence of H_2. To extend this analysis, the rate of the isotopic exchange between H_2 and D_2, namely,

$$H_2(g) + D_2(g) \rightarrow 2HD(g), \quad (2)$$

was measured simultaneously with the exchange in reaction (1). ZnO was chosen as a catalytic agent for reaction (1) and (2). The choice was suggested by past studies (*2*), which have shown that solid-state additions to ZnO influence its catalytic activity for reaction (2). Thus, if H_2 adsorption is kinetically significant in the $CO + H_2$ reaction, the rate of the latter should be influenced by additions to ZnO. Furthermore, it has been reported that on ZnO the product distribution from $CO + H_2$ mixtures is a function of the redox level of the oxide (*3*); the effect has been traced to different adsorption modes of CO which are related to redox conditions of the ZnO surface. On a broader perspective, a knowledge of the adsorption characteristics of catalytically reacting $CO + H_2$ and the role of the former in the formation of hydrocarbons versus oxygenated products seems to be an essential prerequisite toward building a satisfactory model for the $CO + H_2$ synthesis reaction and for deriving predictive correlations for technological applications.

TABLE 1

Chemical Composition, BET Surface Area, and Excess Zinc for ZnO Samples

Sample	Addition[a] (at%×10²)	Surface area (m^2/g)	Excess zinc[b] (ppm by wt)
Series A			
ZnO + Ga	0.69	0.53	3.0
ZnO + Ge	4.82	2.49	5.4
ZnO + Li	43.4	0.20	10
ZnO + Re	0.96	0.69	3.6
Series B			
ZnO	—	1.09	10
ZnO + K[c]	4.58	0.86	3.5
ZnO + Cr[c]	11.8	2.05	—[c]
ZnO + Cu	10.5	2.10	21
ZnO + Fe	9.98	1.99	1.2
ZnO (Kadox)	—	0.35	—

[a] By absorption spectroscopy.
[b] ±0.1 ppm.
[c] No analysis possible due to Cr in sample.

EXPERIMENTAL

ZnO samples were prepared in two batches. In one batch, ZnO (Merck, ACS reagent) was slurried with the appropriate amount of a metal nitrate solution, dried, and heated at 850°C in air for 6 hr (Series A). In a second batch, $Zn(CO_3)_2$ was precipitated from $Zn(NO_3)_2 \cdot 6H_2O$, (Erba, c.p.), washed, slurried with a metal nitrate solution (or KOH for ZnO + K), dried, ball milled, and heated at 800°C for 3 hr in air. The ball milling and heating sequence was repeated for an additional 3 hr (Series B). A sample of ZnO (Kadox, N.J. Zinc Co.) was also employed. Sample homogeneity was checked by chemical analysis on different aliquots of the same sample. Chemical composition and BET surface area of the ZnO preparations are reported in Table 1.

Bulk characterization of the ZnO samples was carried out by X ray, and chemical

analysis was used to determine the stoichiometric Zn excess (*4*), while surface composition was measured by Auger spectroscopy (Physical Electronics Industries) using a 3-keV electron beam, a 50-A current, a 3-V modulation amplitude, and a time constant of 0.001 sec. Surface composition was calculated by means of the equation,

$$C_X = [(H_X/f_X)/(\sum_n H_n/f_n)] \times 100,$$

where C_X is the atom percentage of element X (O, Zn); H_X and f_X are the peak height and sensitivity factor for X. $^{13}C^{16}O$, 90.5 at% ^{13}C (Merck, Sharp, and Dhome), and $^{12}C^{18}O$, 99.8 at% ^{18}O (Gesellschaft fur Kernforschung, Karlsruhe) were diluted with high-purity He, H_2, D_2, and N_2 as needed. The gas mixture was used without further purification. A typical isotopic feed composition was (percentage, v/v): $^{12}C^{16}O$, 4.75; $^{13}C^{16}O$, 45.2; $^{12}C^{18}O$, 49.95; $^{13}C^{18}O$, <0.1. For reaction (2) the ratio $D_2/H_2 = 0.05$ was used throughout. By suitable additions of He, all runs were made at a total pressure of 250 Torr. The rate of reaction (1) was followed in an all-glass system having a total volume of 300 cm^3 and including the reactor, a recycle loop, and a magnetically driven pump. Gas samples were periodically withdrawn and analyzed by mass spectrometry (EAI 250B).

Generally, 0.5 g of catalyst (35–50 mesh) was diluted to 3 cm^3 with Al_2O_3 (Alcoa Tab T61) and loaded into the reactor, heated in O_2 (200 Torr) at 400°C for 10 min, and evacuated. The pretreatment was repeated twice, followed by cooling to reaction temperature. These conditions were found by ir spectroscopy to clean effectively the adsorbed ZnO surface of CO. With the enriched CO samples employed it was convenient to follow the course of the reaction by monitoring the ratio of mass 30 to mass 31; this ratio decreased from the initial value of 20 to about 1 at equilibrium, thus providing an accurate ($\pm 1\%$) record of the mass ratio as a function of time. Reaction conversions of 70 to 80% were easily followed. Partial pressures of CO ranged between 6 and 100 Torr. In all ZnO preparations an initial period of time-dependent reaction rate was observed in the case of reaction (2). The length of this period decreased with increasing number of reruns, until it disappeared altogether for a sufficiently large number of runs. The presence or the length of the initial transient period did not influence the value of the steady rate. To eliminate this effect, prior to each run ZnO samples were treated at 400°C, evacuated ($<10^{-3}$ Torr) for 2 hr, and cooled to 300°C; 300 Torr of H_2 was admitted and then evacuated ($<10^{-3}$ Torr), and the reaction mixture was introduced. No reaction on the Al_2O_3 diluent or reactor walls was detected at 300°C. At this temperature the reaction rate was found to be independent of the speed of the recycle pump when operated between 9 and 90 liters/hr, with the latter rate being employed for all runs. The reaction rate was not influenced by the sequence with which the partial pressure of CO was varied. No formation of CO_2 or other products (alcohols) was detected in either the presence or absence of H_2. A few measurements on CO adsorption were carried out in a conventional volumetric apparatus employing a capacitance pressure gauge. Gas samples were analyzed at the end of the adsorption runs and no CO_2 was detected.

An estimate of the error in the kinetic parameters gave $\pm 30\%$ for k° and approximately $\pm 15\%$ for m, n, and z. These estimates were confirmed experimentally.

RESULTS

Characterization of ZnO Samples

For all samples investigated X-ray diffraction showed the presence of one phase only and no appreciable deviation from the literature value of the unit cell param-

eter of ZnO (3.249 Å). The results of the excess Zn analysis are reported in Table 1. The effect of Li in increasing the excess Zn concentration is well known, whereas that of Cu may be rationalized assuming that Cu was dissolved in ZnO as Cu_2O. Surface analysis by Auger spectroscopy is reported in Table 2.

The data in Table 2 reveal two significant effects. Surface concentration of the additions was about two orders of magnitude larger than bulk concentration (Table 1), and the Zn/O ratio ranged from 1.11 to 1.39 for Series A samples and from 2.22 to 2.44 for Series B samples, whereas a value of 0.84 was found for ZnO Kadox. The reported high values for the Zn/O ratio falling in two distinct ranges for the two series of samples indicate that the effect of the addition on the surface stoichiometry was secondary to that of the preparative conditions. ZnO Kadox, which is obtained by direct oxidation of Zn metal, had probably been subjected to higher temperatures than those experienced by Series A and B samples. This is reflected in a Zn/O ratio closer to the correct bulk stoichiometry. In the calculation of the Zn/O ratios reported in Table 2 an Auger sensitivity factor for Zn of 0.435 (referred to a sensitivity factor of 1 for oxygen) was employed, instead of the more common value of 0.350. The value of 0.435 was obtained by means of measurements on the $(11\bar{2}0)$ face of single-crystal ZnO, the Zn/O ratio of which is 1. Consequently, the Zn/O values reported in Table 2 represent a lower limit for the Zn content. The high Zn content at the surface is unexpected since it cannot be the result of electron beam damage. In fact no change in the Zn/O ratio with time was noticed and the majority of past studies confirm the stability of ZnO surfaces under Auger conditions (*5*). Indeed, the large difference in the Zn/O ratio among the samples is not consistent with an unstable ZnO surface; specifically, ZnO Kadox should not have shown an oxidized surface. One sample from Series A and one sample from Series B were submitted to Auger surface analysis after their use as catalysts for reaction (1). No substantial difference in the Zn/O ratio, as recorded prior to reaction, was discovered. Auger analysis also indicated the presence of C and S, the concentration ($\approx$5 atom%) of which was nearly constant for all the ZnO preparations.

TABLE 2

Surface Composition of ZnO Samples

Sample	Addition (at%)	Zn/O
Series A		
ZnO + Ga	—[a]	1.28
ZnO + Ge	2.9	1.35
ZnO + Li	—[b]	1.11
ZnO + Re	4.0	1.39
Series B		
ZnO	—	2.38
ZnO + K	1.3	2.38
ZnO + Cr	3.9	2.22
ZnO + Cu	—[c]	2.27
ZnO + Fe	3.1	2.44
ZnO (Kadox)	—	0.84

[a] Concentration too low for detection.
[b] No reference spectra available.
[c] A 920-eV peak overlaps with Zn peak.

Isotopic Mixing in Carbon Monoxide

The derivation of the rate equation for reaction (1) was carried out assuming a sequence of two adsorption–desorption reaction steps, namely,

$$^{13}C^{16}O(g) + {}^{18}O(s) \rightarrow {}^{13}C^{18}O(g) + {}^{16}O(s) \quad (1a)$$

$$^{12}C^{18}O(g) + {}^{16}O(s) \rightarrow {}^{12}C^{16}O(g) + {}^{18}O(s) \quad (1b)$$

$$^{13}C^{16}O(g) + {}^{12}C^{18}O(g) \rightarrow {}^{13}C^{18}O(g) + {}^{12}C^{16}O(g) \quad (1)$$

where s refers to the adsorbed phase. Since

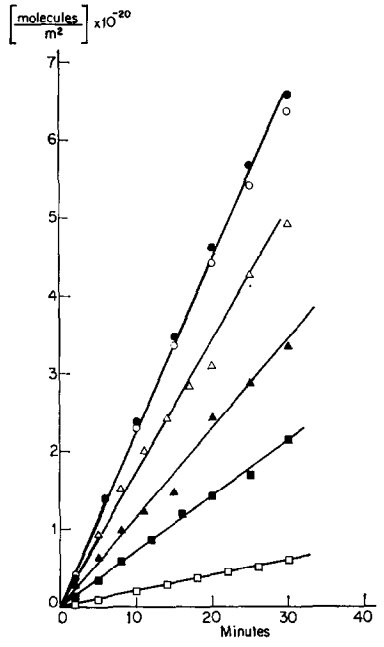

FIG. 1. Conversion versus time for reaction (1) on ZnO + K at 300°C. p_{CO} (Torr): (●, ○) 81.0, (△) 54.3, (▲) 39.1, (■) 21.5, (□) 6.6.

the reacting system is at equilibrium, the rates of reaction steps (1a) and (1b) are similar to the rate of the overall equilibration reaction (1). Neglecting kinetic isotope effects and gas–solid oxygen exchange and considering reaction step (1a), the rate is given by the expression,

$$-\frac{1}{w}\frac{V}{RT}\frac{dp_{29}}{dt} = k'_c p_{29} - k_c{}^b p_{31}, \quad (3)$$

where w, V, R, T, p_{29}, k'_c, and $k_c{}^b$ are the catalyst weight, volume of the catalyst bed, gas constant, reactor temperature, partial pressure of $^{13}C^{16}O$, and rate coefficients, respectively, of forward and reverse reaction step (1a). The rate coefficients, k'_c and $k_c{}^b$ are dependent upon temperature and p_{29}. After introducing the molar fraction of $^{13}C^{16}O$, $x_{29} = (p_{^{13}C^{16}O})/(p_{CO})_{total}$, eliminating $k_c{}^b$ by means of the equilibrium conditions, $k'_c(p_{29}) = k_c{}^b(p_{31})_\infty$, and integrating and solving for k'_c, Eq. (3) yields

$$k'_c = \frac{2.3V}{wRTt}\beta_\infty \log\frac{1}{1-\alpha_c} \quad (4)$$

[expressed in moles per (grams of catalysts · atmospheres · minutes)], where $\beta_\infty = (p_{31}/p_{29}{}^0)$ and the conversion,

$$\alpha_c = \frac{\beta - \beta_0}{\beta_\infty - \beta_0} = \frac{(x_{29})_0 - (x_{29})_t}{(x_{29})_0 - (x_{29})_\infty} = \frac{(x_{31})_t - (x_{31})_0}{(x_{31})_\infty - (x_{31})_0}. \quad (5)$$

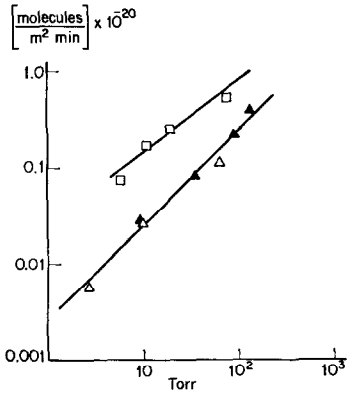

FIG. 2. Rate v_c for reaction (1) versus p_{CO} on ZnO Kadox (▲), ZnO + Ga (△), and ZnO + Ge (□) at 300°C.

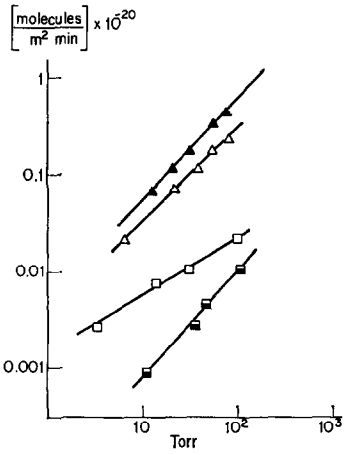

FIG. 3. Rate v_c for reaction (1) versus p_{CO} on ZnO (▲), ZnO + Li (□) ZnO + Ge (■) and ZnO + K (△) at 300°C.

The subscripts ∞, o, and t refer to values at equilibrium, at the start, and at time t, respectively. The experimental measurements were carried out by recording the ratio $\gamma = x_{30}/x_{31}$ as a function of time. Since

$$\frac{\gamma_t - \gamma_\infty}{\gamma_t + 1}\frac{\gamma_o + 1}{\gamma_o - \gamma_\infty} = \frac{(x_{31})_\infty - (x_{31})_t}{(x_{31})_\infty - (x_{31})_o} = 1 - \alpha_c,$$

from the known values of the conversion, α_c, could be calculated. If A is the catalyst specific surface area, the reaction rate v_c is given (in molecules per square meters ·minutes) by

$$v_c = \frac{k'_c N_A}{A} p_{CO}, \qquad (6)$$

where N_A is Avogadro's number. Typical results, expressed as $\{(2.3V)/(wRT)(\beta_\infty) \log [1/(1 - \alpha_c)]\}$ versus time, are reported in Fig. 1.

By performing experiments at different p_{CO} it was found that v_c was not always a first-order rate as expressed in Eq. (6). The experimental results on the influence of p_{CO} on v_c are collected in Figs. 2 and 3.

To test the effect of the presence of H_2 on the rate of reaction (1) runs were performed at 300°C with a premixed mixture of CO and $H_2 + D_2$. The results of this set of runs are reported in Figs. 4 and 5.

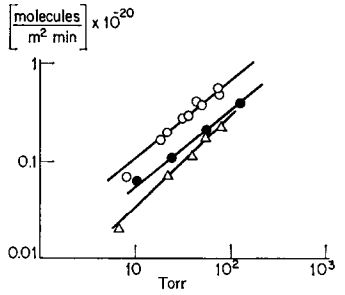

FIG. 4. Rate v_c for reaction (1) versus p_{CO} on ZnO + K at 300°C. (△) No H_2; (●) 50% (v/v) H_2; (○) 75% (v/v) H_2.

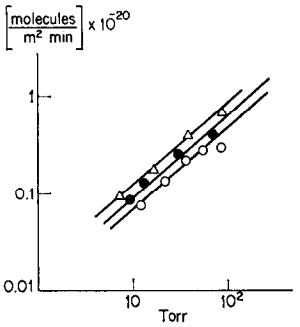

FIG. 5. Rate v_c for reaction (1) versus p_{CO} on ZnO + Cr at 300°C. (○) No H_2; (●) 50% (v/v) H_2; (△) 75% (v/v) H_2.

No formation of H_2O was detected in these runs. At 300°C the presence of H_2O in the reacting mixture had a strong inhibiting influence on the rate of reaction (1). After H_2O inhibition, original activity could be recovered by subsequent treatment with O_2 (Table 3).

Employing a commercial methanol synthesis catalyst (ZnO–Cr_2O_3, specific surface area: 76 m^2/g) under conditions of temperature and p_{CO} similar to those employed for the ZnO samples, isotopic equilibrium in reaction (1) was attained in <2 min.

Oxygen Exchange between CO and ZnO

Early in this study it became clear that oxygen exchange between CO and ZnO took place. Although the extent of the exchange was not sufficient to produce

TABLE 3

Effect of H_2O on the Rate of Reaction (1) on ZnO + K at 300°C, p_{CO} = 95.5 Torr, and Total Pressure = 250 Torr

Gas-phase composition	v_c [(molecules/m^2 min) $\times 10^{-20}$]
CO + He	0.575
CO + He + H_2O (8.5 Torr)	0.0022
CO + He[a]	0.75

[a] After pretreatment, O_2, 400°C, 10 min.

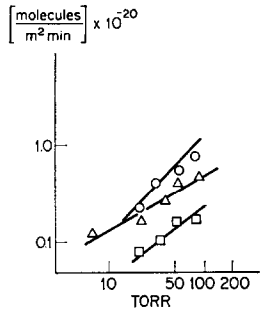

FIG. 6. Rate v_o for reaction (6) versus p_{CO} at 300°C. ZnO (○); ZnO + Cr (□); ZnO + K (△).

noticeable deviations from the linear conversion plots (Fig. 1), it was nevertheless deemed of interest to quantify the effect for its possible implications in the elucidation of the details of CO adsorption at ZnO surfaces. The rate of the exchange reaction,

$$^{12}C^{18}O(g) + Zn^{16}O \rightarrow {}^{12}C^{16}O(g) + Zn^{18}O, \quad (7)$$

was expressed as the difference between the rate of disappearance of $^{12}C^{18}O$, or

$$dp_{30}/dt = k_{30}p_{30} - k'_{28}p_{28}, \quad (8)$$

and the rate of appearance of $^{13}C^{18}O$ [Eq. (3)]. By means of Eq. (4) and the integrated expression of Eq. (8), the forward rate coefficient of Eq. (7), k_o, is given (in moles per grams of catalyst ·atmospheres·minutes) by

$$k_o = k_{30} - k_{31} = -\frac{2.3V}{wRT}\left[(x_{30})_\infty \log\frac{1}{1-\alpha_{30}} + (x_{31})_\infty \log\frac{1}{1-\alpha_{31}}\right], \quad (9)$$

where α_{30} and α_{31} are the reaction conversions corresponding to mass 30 and 31, respectively. Finally, the rate of reaction (7) is given (in molecules per square meters ·minutes) by

$$v_o = \frac{k_o N_A}{A} p_{CO}. \quad (10)$$

Since multiple exchange ($^{13}C^{18}O$–ZnO) was not considered in the derivation of Eq. (9), the latter is strictly valid at $t = 0$ only. However, no significant deviation from straight-line plots was observed even at moderate conversion. The experimental results of the effect of p_{CO} on the rate of reaction (7) are reported in Figs. 6 and 7.

H_2–D_2 Equilibration

The rate of the isotopic equilibration between H_2 and D_2 was derived in a manner similar to that employed for reaction (1). Assuming that only adsorption and desorption steps are kinetically significant, namely,

$$D_2(g) \rightarrow 2D(s) \quad (11a)$$

$$H_2(g) \rightarrow 2H(s) \quad (11b)$$

$$2D(s) + 2H(s) \leftrightharpoons 2HD(g) \quad (11c)$$

$$D_2(g) + H_2(g) \rightarrow 2HD(g) \quad (11)$$

the rate of reaction (11a), which is similar to the rate of reaction (11), is given by

$$-\frac{V}{wRT}\frac{dp_{D_2}}{dt} = k'_D p_{D_2} - k_D{}^b, \quad (12)$$

where k'_D and $k_D{}^b$ are the forward and reverse rate coefficients of reaction step (11a) and p_{D_2} is the D_2 partial pressure. Introducing the reaction conversion,

$$\alpha_D = [(x_{HD})_t - (x_{HD})_o]/[(x_{HD})_\infty - (x_{HD})_o],$$

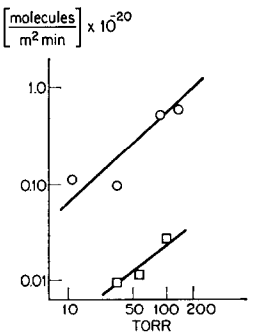

FIG. 7. Rate v_o for reaction (6) versus p_{CO}. ZnO + Ga (○); ZnO + Re (□).

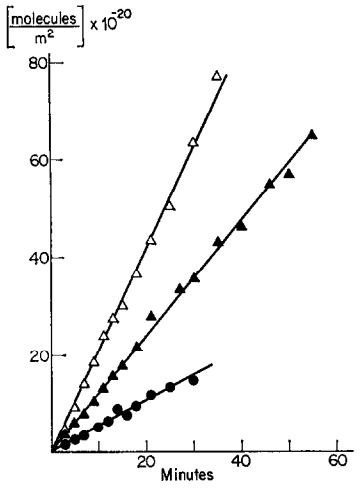

FIG. 8. Conversion versus time for reaction (11) on ZnO + K at 300°C. p_{H_2} (Torr): (●) 31.5; (▲) 71.7; (△) 196.

where x_{HD} is the mole fraction of HD; eliminating $k_D{}^b$ and integrating, Eq. (12) yields

$$k'_D = [(2.3V)/(wRTt)] \log [1/(1 - \alpha_D)].$$

The rate of reaction (11) is given (in molecules per square meters·minutes) by

$$v_D = (k'_D/A)N_A p_{H_2}. \qquad (13)$$

Linear plots of

$$[(2.3V)/(wRT)] \log [1/(1 - \alpha_D)]$$

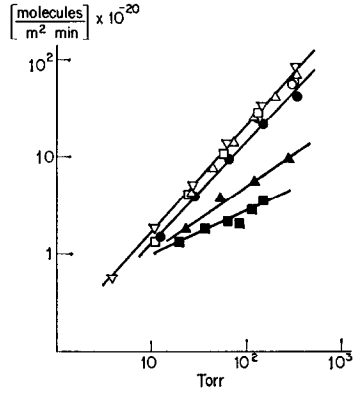

FIG. 9. Rate v_D for reaction (11) on ZnO versus $(p_{H_2})_t$ at 300°C. (○, △, ▽) Different runs under similar conditions, no CO; (□) 0.36% (v/v) CO; (●) 2.5% (v/v) CO; (▲) 24% (v/v) CO; (■) 51% (v/v) CO.

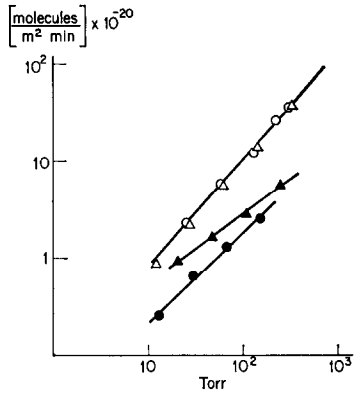

FIG. 10. Rate v_D for reaction (11) versus $(p_{H_2})_t$ on ZnO + Cr_2O_3 at 300°C. (○) No CO added; (△) 0.4% (v/v) CO; (▲) 25% (v/v) CO; (●) 50% (v/v) CO.

versus time were obtained in all cases (Fig. 8). On the basis of the available experimental results it was not possible to distinguish meaningfully between reaction scheme (11) and alternate adsorption–desorption reaction sequences.

The results on ZnO, ZnO + K, ZnO + Cr, and ZnO + Cu, plotted according to Eq. (13) at different $(p_{H_2})_t$ and 300°C, are reported in Figs. 9, 10, and 11, which include information on the effect of CO on the rate of reaction (11). H_2O was found to have an inhibiting effect; 0.1% D_2–H_2O exchange was also detected.

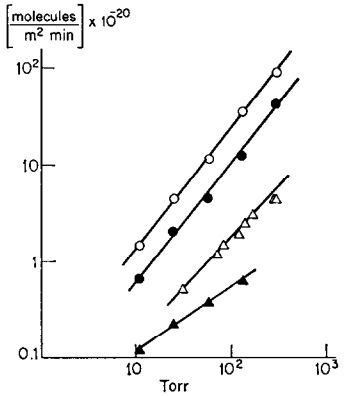

FIG. 11. Rate v_D for reaction (11) versus $(p_{H_2})_t$ on ZnO + K at 300°C. (○) No CO added; (●) 0.4% (v/v) CO; (△) 25% (v/v) CO; (▲) 50% (v/v) CO.

TABLE 4

Values of the Constants $k_c°$, $k_o°$, m_c, and m_o in Eqs. (14) and (15) for Reactions (1) and (7) on ZnO at 300°C

Sample	$k_c°$[a]	m_c	$k_o°$[a]	m_o
Series A				
ZnO + Ga	2.1	0.90	2.0	0.90
ZnO + Ge	3.3	0.70	~1.0	0.70
ZnO + Li	0.2	0.65	—	—
ZnO + Re	0.1	0.75	0.1	0.75
Series B				
ZnO	2.0	1.0	0.8	0.90
ZnO + K	2.1	1.0	1.50	0.58
ZnO + Cr	2.0	1.0	0.75	0.61
ZnO + Cu	>6	~1.0	>6	~0.65
ZnO + Fe	3.0	1.35	~0.5	~1.0
ZnO Kadox	1.9	0.90	~ 1.70	0.42

[a] Expressed as (molecules per square meters·minutes·atmospheres) $\times 10^{-20}$.

DISCUSSION

CO Isotopic Equilibration

The results reported in Figs. 2 to 7 for reactions (1) and (7) may be expressed by equations of the type,

$$v_c = k_c° p_{CO}^{m_c} [\text{reaction (1)}] \quad (14)$$

and

$$v_o = k_o° p_{CO}^{m_o} [\text{reaction (7)}], \quad (15)$$

where $k_c°$, $k_o°$, m_c, and m_o are constants. The calculated values of the constants are reported in Table 4. Inspection of Table 4 shows that Series A and B samples fall kinetically into two separate groups. In fact, while in samples of Series A the pressure dependence of the rates of reactions (1) and (7) was similar, this was not the case for Series B samples. Furthermore, the values of $k_c°$ and $k_o°$ are numerically closer for Series A than for Series B samples. Despite uncertainty in some of the numerical values the difference in kinetic behavior between the two series is striking. We suggest that this effect is an indication that, for Series A samples, the isotopic mixing reaction (1) took place through alternate oxygen exchange steps, similar to reaction (7), whereas a reaction sequence not directly involving the oxygen of ZnO was responsible for reaction (1) catalyzed by Series B samples. To develop this conclusion further the information in Table 2 is instructive. In fact, a consistent difference in the Zn/O surface ratio was present in the two sets of samples. To trace the origin of this variation, AES measurements of the Zn/O ratio were conducted on selected faces of single-crystal ZnO under conditions similar to those employed for powdered samples (Fig. 12). It was found that samples of Series A and Kadox had a surface Zn/O ratio intermediate between those of the $(10\bar{1}0)$, $(11\bar{2}0)$, and $(000\bar{1})$ crystal faces, whereas samples of Series B exhibited a value close to that of the

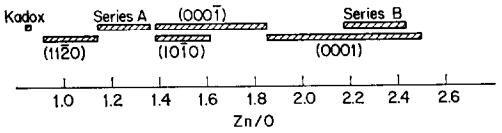

FIG. 12. Surface Zn/O ratio for polycrystalline ZnO and single-crystal ZnO faces.

(000$\bar{1}$) crystal face. It is suggested that the Zn/O ratio was mostly the result of the time–temperature schedule followed during sample preparation. The suggestion was tested directly by measuring the ratio on a fresh ZnO sample (Merck) and obtaining a value of 2.32. Upon heating at 800°C the ratio decreased to 1.49. It is also reasonable to assume that morphological conditions (i.e., different surface planes) aided in the stabilization of the varying ratios. There is, in fact, already evidence that Cu additions enhance the appearance of basal planes at ZnO surfaces (*6*).

Reaction steps for reaction (1) may include the dissociative adsorption of CO followed by recombination and desorption. Reaction (1) may also occur through the formation and decomposition of a surface adsorbate in alternate reduction and oxidation stages. For the latter reaction sequence participation of oxygen from ZnO is essential and, consequently, the exchange of oxygen between CO and ZnO [reaction (7)] becomes an integral part of this reaction scheme. Alternatively, CO may be adsorbed with the formation of associative complexes containing two or more CO molecules and desorbed following decomposition of the complex.

Because of the high dissociation energy of CO (255 kcal/mole) dissociative chemisorption is unlikely to be a major contributing factor to reaction (1) at 300°C.

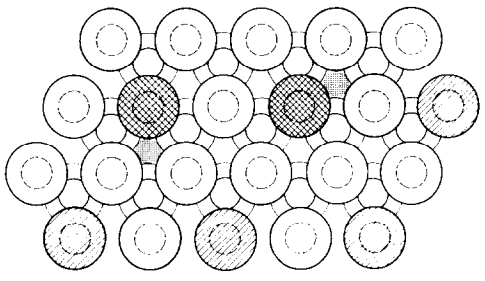

FIG. 13. Schematic view of CO chemisorption on the (000$\bar{1}$) plane of ZnO. (○) Topmost layer of Zn; (○) second oxygen layer, (◌) second Zn layer; (▨) oxygen vacancy, (●, ◍) adsorbed CO.

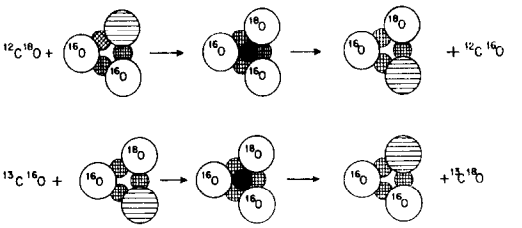

FIG. 14. Models for reactions (1) and (6) at the (000$\bar{1}$) surface plane of ZnO. (●) Carbon, (◉) zinc, (○) oxygen, (◍) oxygen vacancy.

Two-site associative adsorption seems a logical candidate and a physically plausible adsorption precursor for reactions (1) and (7). Molecular orbital considerations of the electronic configuration of the CO molecule do not in fact preclude the possibility of a bridged binding, or of any scheme involving both C and O bonded to the surface (*7*).

A likely candidate for a site pair on the (000$\bar{1}$) face for the adsorption of CO is the combination of the hole with threefold oxygen coordination and a neighboring oxygen vacancy (Fig. 13). The course of reaction (1) on this plane may be visualized as a sequence of adsorption and desorption steps, similar to those postulated for reaction (7) (Fig. 14). On this surface-reactive CO, adsorption takes place on a surface essentially uncovered by CO; assuming, then, a Langmuir formulation for CO adsorption the values of m_c and m_o should be in the range $0 < m < 1$. This is consistent with the values found experimentally (Table 5). On the other hand, it is suggested that CO adsorption on the more reduced surfaces of Series B samples takes place on a surface largely covered by CO; the isotopic mixing reaction (1) thus follows a path which includes the formation and decomposition of surface CO complexes, kinetically distinct from the path leading to reaction (7). Furthermore, it may be argued that, again following a Langmuir formalism for the associative CO adsorption, the values of m should be in the range $1 < m < 2$. This is

TABLE 5

Effect of H_2 on the Rate Constant, $k_c°$, and Exponent m_c, from Eq. (14) for Reaction (1) Catalyzed by ZnO, Series B, at 300°C

Sample	p_{H_2}/p_{CO}	$k_c°$ [(molecules/ m^2 min atm^{m_c}) $\times 10^{-20}$]	m_c
ZnO	—[a]	2.0	1.00
	0.96	0.33	0.31
	2.94	1.43	0.66
ZnO + K	—[a]	2.1	1.00
	1	1.65	0.80
	3.03	3.25	0.80
ZnO + Cr	—[a]	2.0	1.00
	1	3.6	0.84
	3.03	4.7	0.85
ZnO + Cu	—[a]	>6.0	—
	0.5	0.128	0.32
	1	0.095	0.15

[a] CO only.

consistent with the experimental values reported in Table 4. It is worth noting that from studies on reaction (1) catalyzed by metallic surfaces, it was concluded that associative CO adsorption played the major role (*8*). In this instance the adsorption intermediate may be looked upon as a head-to-tail square complex with the participation of two electrons per complex derived from and shared with the surface pair site. π bonding with the surface sites would be involved, and electrons from the metal would enter the $2p_z$ CO orbitals, resulting in a weakened C–O bond.

No clear pattern emerged on the role of solid additions to ZnO on the rate of reaction (1) (Table 4). The surface Zn/O ratio seemed to be the crucial factor. If the redox conditions of the ZnO surface played a central role, it was reasoned that variations in the nature of the controlling adsorption isotherm should also be observed whenever surface redox level was modified by the presence of gas-phase species, which would interact with the surface oxygen. H_2 is an obvious candidate for this test, since it is known that the reduction rate of powdered and single-crystal ZnO is faster in H_2 than in CO (*9*). The results of the effect of H_2 are collected in Table 5.

Inspection of Table 5 shows that the adsorption of CO was indeed modified by the presence of H_2, as indicated by a gradual decrease of m_c as p_{H_2} increased. If two-site CO adsorption becomes preponderant as a result of increased oxygen vacancies at the surface, the introduction of the Langmuir factor $(1 - \theta)$ (*2*) in the rate expression has the result of lowering the value of m. The presence of H_2 did not have a drastic influence on $k_c°$; there was some evidence, though, for a higher rate of reaction (1) on ZnO + Cr and ZnO + K (Figs. 4 and 5), an effect of H_2 on the strength of the C–O bond in adsorbed CO. This is known to occur on several transition metal catalysts (*10*). The strong inhibition of H_2O in reaction (1) may be related to the formation of surface groups,

$$\begin{matrix} OH- & H+ \\ | & | \\ Zn^{+2} & O^{-2}, \end{matrix}$$

the presence of which is supported by ir observations (*11*).

H_2–D_2 Exchange

The rate of reaction (11) was expressed as

$$v_C = k_h^\circ p_{H_2}^{m_H}, \qquad (16)$$

where k_h° and m_H are constants. The computed values of the constants are collected in Table 6. A number of points of interest emerge from the results of Table 6. Reaction (11) was influenced by solid-state additions to ZnO, the activity sequence being ZnO + K ≈ ZnO + Cu > ZnO > ZnO + Cr. This is the result expected from simple considerations of the effect of the additions on the concentration of surface defects in ZnO. The activity results further confirm earlier studies (*2*) and the model for reaction (11), which include the presence of surface cations abnormally charged (Zn^+) or anions foreign to the lattice (OH^-).

Values of $m_H > 1$ are an indication that the reactive H_2 adsorption took place on sites covered by H_2. This is consistent with the observation that the rate of reaction (11) increased with p_{H_2} (Figs. 9–11). A further interesting point is the inhibition of reaction (11) by CO, indicating a strong competition by CO surface sites for reaction (11). This is in agreement with the earlier conclusion of the absence of drastic influence of H_2 on the rate of reaction (1). Furthermore, when measured in the absence of H_2 the rate of reaction (1) was slower than that of reaction (11); however, due to the influence of CO on the H_2–D_2 equilibration, the rates of reaction (1) and (11) become comparable for p_{H_2}/p_{CO} ratios <1. Thus in CO + H_2 synthesis on ZnO for low p_{H_2}/p_{CO} ratios neither CO nor H_2 adsorption must be the controlling step. This disagrees with earlier work indicating the adsorption of H_2 as the limiting step in the synthesis of methanol from CO + H_2 on ZnO (*12*).

Turnover Rate and Reaction Efficiency

The number of active sites per unit surface area, ϕ, was determined from knowl-

TABLE 6

Rate Constant, k_H°, and Exponent m_H in Eq. (16) for Reaction (11) Catalyzed by ZnO, Series B, at 300°C

Sample	p_{H_2}/p_{CO}	k_H° [(molecules/ m^2 min atm^z) × 10^{-20}]	m_H
ZnO	—[a]	185	1.1
	39	116	1.05
	3.16	20	0.67
	0.96	6.9	0.45
ZnO + K	—[a]	290	1.25
	249	123	1.3
	3.0	15	0.93
	1.0	2.1	0.66
ZnO + Cr	—[a]	93	1.1
	3	11.7	0.71
	1	6.4	0.62
ZnO + Cu	—[a]	265	1.58
	302	83	1.32
	39	39	1.02
	2.9	3.7	0.65
	1.0	2	0.38

[a] No CO present.

edge on the amount of solid–gas oxygen exchange (*13*). If Z is the atom fraction of ^{18}O in the gas phase [i.e., $(N_{30} + N_{31})/N_T$, N, number of molecules] and $(v_g)_i$ and $(v_g)_\infty$ are the volume percentages of ^{18}O present in the gas phase initially and at a time in which the oxygen isotopic equilibrium between gas and solid is reached, respectively, a mass balance of ^{18}O between gas and adsorbed phases gives

$$Z[(v_g)_i - (v_g)_\infty] = 2A\phi[(c_s)_\infty - (c_s)_i], \quad (17)$$

where A, $(c_s)_\infty$, and $(c_s)_i$ are the surface area available, the surface concentration of ^{18}O at equilibrium, and the initial concentration, respectively. The derivation assumes that each surface site contains on the average two exchangeable oxygens and that isotopic equilibrium between gas and surface is reached by the time an analysis is made. This equilibrium condition was experimentally verified. Values of ϕ were calculated from Eq. (17) and used in the computation of the turnover rate

$$\dot{N} = v_c/\phi. \quad (18)$$

The values are reported in Table 7.

The values of ϕ show that reactions (1) and (7) were confined to a small fraction (0.001) of the ZnO surface, as found previously for several oxides including ZnO (*13*). Furthermore, it is likely that, at the reaction temperature employed, oxygen interchange involved layers below the topmost. If this were the case the actual values of ϕ and those of the resulting surface coverage during reaction were smaller indeed. The values of ϕ were independent of p_{CO}, a likely consequence of the fact that the number of active surface sites was not a fixed fraction of the total number of sites. The collision efficiency of the surface for reaction (1), η, defined by the ratio between the rate v_c, which gives the number of collisions between gaseous CO molecules and the ZnO surface leading to reaction under conditions of ad-

TABLE 7

Fraction of Active Surface, ϕ, Turnover Rate, $\dot{N}$, and Surface Collision Efficiency, η, for Reaction (1) Catalyzed by ZnO at 300°C

Sample	p_{CO} (Torr)	ϕ ($m^{-2} \times 10^{-8}$)	$\dot{N}$ (min^{-1})	η ($\times 10^8$)
ZnO	20.8	2.7	—	0.35
	31.7	2.7	1.6	0.35
	54.7	2.7	3.1	0.39
	75.1	2.7	4.2	0.38
ZnO (Kadox)	10.6	5.5	0.1	—
	63.0	5.5	5.0	—
ZnO + Cr	22.0	2.5	1.2	0.15
	35.9	2.5	2.0	0.16
	54.9	2.5	2.7	0.13
ZnO + Ge	5.9	2.5	0.7	—
	11.0	2.5	1.5	—
	20.0	2.5	2.3	—
ZnO + K	6.6	1.4	0.3	0.19
	21.5	2.7	0.7	0.21
	39.1	2.6	1.1	0.18
	81.0	2.2	2.6	0.18
	8.14	2.2	2.6	0.18
ZnO + Cu	51.8	2.2	43	1.44
	81.6	2.2	107	2.24

sorption–desorption equilibrium (exchange rate), and the total number of collisions, $\dot{n}$, is given by

$$\eta = \frac{v_c}{\dot{n}} = \frac{k_c^{\circ} p_{CO}^{m_c}}{p_{CO}/(2\pi MRT)^{\frac{1}{2}}} = k_c^{\circ} p_{CO}^{m_c-1}(2\pi MRT)^{\frac{1}{2}}, \quad (19)$$

where M is the molecular weight of CO. Values of η are collected in the last column of Table 7. Characteristically, ZnO + Cu preparations had surface efficiencies about one order of magnitude larger than the other samples. η was independent of p_{CO}, indicating that the surface steps leading to reaction (1) involved surface conditions (structural defects, redox ratios) which were not a consequence of the adsorption of CO.

From observations on CO adsorption, we have calculated that $\sim 15 \times 10^{17}$ CO molecules/m^2 were adsorbed at 300°C and 75 Torr of CO. Dividing the number of active sites $\phi = 2.7 \times 10^8$ m^{-2} (Table 7) by this number, a separate calculation of the reactive efficiency of the surface is obtained. The result is $(2.7 \times 10^8)/(15 \times 10^{17}) = 1.9 \times 10^{-8}$, which is within an order of magnitude of the value 0.38×10^{-8} calculated from the rate of reaction (1) (Table 7). Unless the accommodation coefficients were very small, adsorption of CO should not have been rate determining in the formation of the correct reaction complex, i.e., the bombardment rate was sufficient on all samples to account for the observed rate or reaction.

CONCLUSION

On ZnO surfaces the reaction of isotopic mixing in CO followed two distinct paths, characterized by the involvement or non-involvement of the ZnO oxygen. The determining factor appeared to be the surface redox level, as obtained during the preparation of the samples. On an "oxidized" surface, oxide oxygen participation was favored. This is supportive of past ideas on the role of surface oxygen ability in the reactivity of oxide surfaces. On a "reduced" surface, CO complexes built by associative chemisorption provided an alternate reaction path, without the inclusion of oxide oxygen. No correlation was found between the surface Zn/O ratio, the bulk Zn excess, and solid additions to ZnO as expected from simple controlled valency considerations.

It is tempting to relate the conclusions from the analysis of reactions (1) and (7) to the type of product distribution from reacting CO + H_2 mixtures. Broadly the hydrogenation of CO by H_2 may be viewed as a two-stage reaction, the initial one consisting of the nondestructive hydrogenation of the C=O bond leading to the formation of the C–OH group. If the resulting C–O bond is sufficiently stable, further hydrogenation leads to oxygenated products, whereas decreased stability could bring about the splitting of H_2O and the formation of CH_4. Since H_2O is always found to be a reaction product, both alternatives do occur concurrently. The stability of the C–O bond in the adsorbate should be dependent, *inter alia*, upon the adsorption mode of CO and the extent of stabilization of the bond in the presence of adsorbed hydrogen. The adsorbate complex HCOH has been shown to be stabilized by a formation energy of 20 kcal/mole (on Fe) (*14*). If the electron density at the C–O bond in the adsorbate is not high, a second hydrogenation with splitting of the OH group is likely to occur. This is the predominant effect at transition metal surfaces since they cannot easily bring about conditions for electron orbital hybridization in bond formation with CO. Conversely, at metal oxide surfaces with increasing electron delocalization, C–O bond stabilization through the participation of several oxygens in the adsorption complex is possible. This precludes the direct desorption of the complex HCOH with formation of formaldehyde (*15*); further hydrogena-

tion brings about the formation of methanol. Thus, despite the obvious difference in the experimental conditions generally employed for methanol synthesis from $CO + H_2$ the results discussed in the previous sections have implications for the latter reaction. Chemisorption of CO and H_2 does not control synthesis rate. Since, at the synthesis temperature, CH_3OH desorption is not likely to be kinetically significant, the slow determining step appears to be the hydrogenation of the adsorbed CO. The presence of H_2 does modify the catalytic activation of CO. The tendency is for the hydrogen chemisorption to increase, structurally and energetically, the interaction of the adsorbed CO with the ZnO surface, a situation reminiscent of the effect of H_2 on N_2 chemisorption on synthetic ammonia catalysts. Despite the inability to define precisely the structural aspects of the role of H_2, the present results establish the kinetic effect of H_2. Selectivity to the formation of CH_3OH is likely to depend upon the stalilization of a low Zn/O ratio at the surface during the prevailing reducing conditions of the synthesis. Consequently, catalyst aging, i.e., increased production of CH_4, may be related to slow surface reduction.

ACKNOWLEDGMENT

One of us (G. Parravano) acknowledges with thanks partial support of this study from the National Science Foundation through Grant No. ENG 75-14193.

REFERENCES

1. Nekipelov, V. N., and Kasatkina, L. A., *Kinet. Catal.* **11**, 751 (1970).
2. Molinari, E., and Parravano, G., *J. Amer. Chem. Soc.* **75**, 5233 (1953).
3. Voroshilov, I. G., Roev, L. M., Kozub, G. M., Lunev, N. K., Pavlovskii, N. A., and Rusov, M. T., *Exp. Theor. Chem.* **11**, 256 (1975).
4. Norman, A., *Analyst* **89**, 261 (1964).
5. Chung, M. F., and Farnsworth, H. E., *Surface Sci.* **22**, 93 (1970); Levine, J. D., and Willis, A., *Surface Sci.* **29**, 144 (1972); Fiermans, L., Arijs, E., Vennik, J., and Maenhout-van der Vorst, W., *Surface Sci.* **39**, 357 (1973); Hopkins, B. J., Leysen, R., and Taylor, P. A., *Surface Sci.* **48**, 486 (1975); Van Hove, H., and Leysen, R., *Phys. Status Solidi* **9**, 361 (1972); Margoninski, Y., and Kirby, R. E., *J. Phys. Chem.* **8**, 1516 (1975); Gopel, W., *Ber. Bunsenges. Phys. Chem.* **80**, 481 (1976).
6. Klier, K., and Kobylinski, T. P., Paper No. 14.6, presented at the Fifth North American Meeting of the Catalysis Society, Pittsburgh, April 1977.
7. Coulson, C. A., "Valence," p. 222. Oxford University Press, New York, 1961.
8. Madey, T. E., Yates, J. T., Jr., and Stern, R. C., *J. Chem. Phys.* **42**, 1372 (1975); Zhdan, P. A., Boreskov, G. K., Boronin, A. I., Egelhoff, W. E., and Vainberg, V. G., *Kinet. Catal.* **18**, 570 (1977).
9. Grunze, M., "Struktur-und Fehlordnungs-Abhangigkeit der Reduktion von Zinkoxidoberflachen mit Kohlenmonoxid und Wasserstoff." Ph.D. Dissertation, Freien Unversitat Berlin, 1977.
10. Dalla Betta, R. A., and Shelef, M., *J. Catal.* **49**, 383 (1977).
11. Kokes, R. J., "Catalysis" (F. Basolo and R. L. Burwell Eds.). Plenum Press, New York, 1973.
12. Leonov, V. E., Karabaev, M. M., Tsybina, E. N., and Petrishcheva, G. S., *Kinet. Catal.* **14**, 970 (1973).
13. Winter, E. S., *J. Chem. Soc.*, 5781, 1964.
14. Kölbel, H., Patzschke, G., and Hammer, H., *Z. Phys. Chem. NF* **48**, 10 (1966); Blyholder, G., and Neff, L., *J. Phys. Chem.* **66**, 1664 (1966).
15. Kölbel, H., and Tillmetz, K. D., *Ber. Bunsenges. Phys. Chem.* **76**, 1156 (1972).